

Automatic Branching Detection in IVUS Sequences

Marina Alberti^{1,2}, Carlo Gatta^{1,2}, Simone Balocco^{1,2}, Francesco Ciompi^{1,2},
Oriol Pujol^{1,2}, Joana Silva³, Xavier Carrillo⁴, and Petia Radeva^{1,2}
`marina.alberti@cvc.uab.es`

¹Dep. of Applied Mathematics and Analysis, University of Barcelona, Spain

²Computer Vision Center, Campus UAB, Bellaterra, Barcelona, Spain

³Coimbra's Hospital Center, Cardiology Department, Coimbra, Portugal

⁴Unitat d'hemodinàmica cardíaca, Hospital universitari "Germans Trias i Pujol",
Badalona, Spain

Abstract. Atherosclerosis is a vascular pathology affecting the arterial walls, generally located in specific vessel sites, such as bifurcations. In this paper, for the first time, a fully automatic approach for the detection of bifurcations in IVUS pullback sequences is presented. The method identifies the frames and the angular sectors in which a bifurcation is visible. This goal is achieved by applying a classifier to a set of textural features extracted from each image of an IVUS pullback. A comparison between two *state-of-the-art* classifiers is performed, AdaBoost and Random Forest. A cross-validation scheme is applied in order to evaluate the performances of the approaches. The obtained results are encouraging, showing a sensitivity of 75% and an accuracy of 94% by using the AdaBoost algorithm.

1 Introduction

Atherosclerosis is an inflammatory process affecting the arterial walls, evolving towards the formation of multiple plaques within the arteries. Atherosclerotic plaques can rupture or grow until they narrow the vessel, potentially leading to complications such as unstable angina, myocardial infarction, stroke and sudden cardiac death. It has been shown that specific vessel locations, such as bifurcations, are critical sites for plaque growth and rupture [1]. The treatment of bifurcations by percutaneous coronary intervention (PCI) represents 20% of all PCI procedures.

Intravascular Ultrasound (IVUS) is a catheter-based imaging technique, generally used for guiding PCI and also as a diagnostic technique. IVUS allows the visualization of high resolution images of internal vascular structures. The procedure for the acquisition of an IVUS sequence consists in inserting an ultrasound emitter, carried by a catheter, into the arterial vessel. The standard IVUS frame is a 360-degree tomographic cross-sectional view of the vessel walls (defined as *short-axis view*), which allows an accurate assessment of vessel morphology and tissue composition. Given a certain angle on the *short-axis view* (see Fig 1-a), the

corresponding *longitudinal view* can be generated by considering the gray-level values of the whole sequence along the diameter at the fixed angle. A typical branching appearance in both *short-axis* and *longitudinal view* is illustrated in Fig 1.

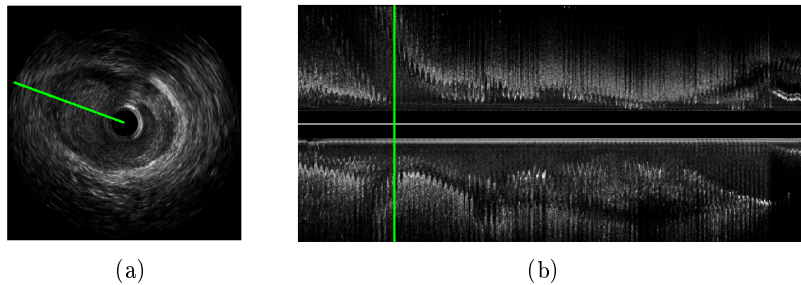


Fig. 1. *Short-axis view* in correspondence of a bifurcation (a); *longitudinal view* of the pullback (b). The two lines indicate the angular and longitudinal bifurcation localizations, in (a) and (b) respectively.

It has been shown that the use of IVUS, compared to the conventional angiography, reduces the four-year mortality in patients in image-guided bifurcation stenting PCI. Although the topic of automatic bifurcation detection has been investigated in several medical imaging modalities, it has never been addressed in IVUS. In this paper, we present, for the first time, a method for the automatic detection of bifurcations in IVUS pullback sequences. In particular, the frames and the angular sectors in which a bifurcation is visible are identified. This goal is obtained by means of a pattern recognition approach, where a set of textural features extracted from each image of an IVUS pullback provides a feature-space in which the classification is performed. The method takes into account several statistical measures computed on the image texture, calculated along the radius of the frames. The classification task is tackled by using the AdaBoost classifier. A comparison with another *state-of-the-art* discriminative classifier, Random Forest, is provided.

The paper is organized as follows: Section II gives an overview of the method, Section III shows the obtained results and Section IV concludes the paper.

2 Method

The method can be divided into two consecutive stages, as illustrated in the block diagram in Fig 2. Firstly, the motion artifacts which affect the IVUS sequence due to heart beating are compensated; then, each angular sector is classified as bifurcation or not.

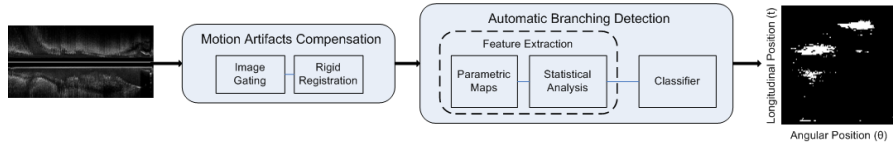


Fig. 2. Block diagram of the proposed approach.

2.1 Motion Artifacts Compensation

During an IVUS pullback acquisition, the catheter is affected by several motion artifacts. The most relevant one is caused by the heart beating, which generates a repetitive longitudinal oscillation of the catheter (swinging effect) along the axis of the vessel, resulting in a possible multiple sampling of the same vessel positions. This undesired effect can be compensated by selecting optimally stable frames, for instance by using an image-based gating technique [2]. Another motion artifact is represented by the catheter fluctuation, causing a spatial misalignment of consecutive frames with respect to the real vessel morphology. In order to align the vessel centers in successive frames, we apply an IVUS registration method [3] consisting in a rigid translation of subsequent frames of the gated sequence. Figure 3 illustrates the output of the two stages.

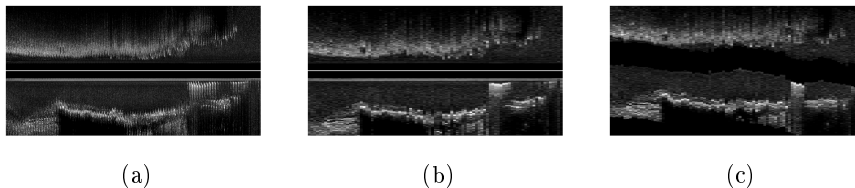


Fig. 3. Longitudinal views of a pullback sequence before motion artifact compensation (a), after the application of the gating technique (b) and after the application of both gating and registration (c), respectively.

2.2 Automatic Branching Detection

In order to identify bifurcations, we define a binary classification problem aimed at distinguishing between the angular sectors of the IVUS frames containing a bifurcation and the others. The angular analysis is justified by the fact that physicians report bifurcation positions in terms of both frame localization and angular extent. The detection task is based on a pattern recognition technique, in which a classifier is first trained by using a database of IVUS sequences manually

labeled by experts and is successively used to identify the presence of a bifurcation in a new frame (test stage). The two main phases of a standard pattern recognition approach are now presented: feature extraction and classification.

Typically, in presence of a bifurcation, the appearance of the visible blood region in a *short-axis* IVUS image tends to an elliptical profile with an eccentricity that is higher with respect to a frame without bifurcation (See Fig. 4-a, -b). The method analyzes radial properties of the vessel texture, for detecting the angular sectors belonging to a bifurcation and in this way it explores the above mentioned eccentricity property. For this purpose, each of the normalized IVUS pullback images $I(x, y) \in [0, 1]$ which constitutes the pullback sequence $S(x, y, t) \in [0, 1]$ is first converted into polar coordinates:

$$\tilde{I}(\rho, \theta) = I(\rho \cos \theta, \rho \sin \theta) \quad (1)$$

where x and y are the horizontal and vertical coordinates in the cartesian system, ρ and θ are the radial and angular coordinates in the polar system (See Fig. 4-c), t is the longitudinal (temporal) coordinate along the pullback.

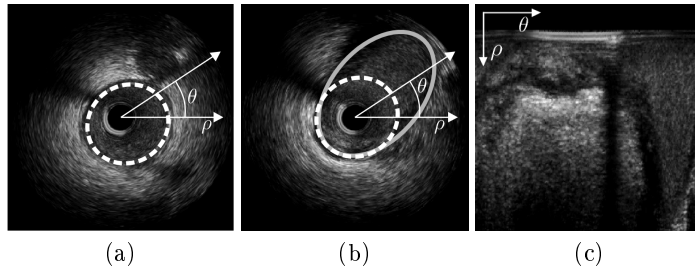


Fig. 4. *Short-axis view* of a non-bifurcation (a) and a bifurcation (b) frame, in cartesian coordinates. The dotted and continuous curves represent an approximation of the typical geometry of the blood region contour in each case. View of the bifurcation frame in the polar representation (c).

A set of N_T texture descriptors is then defined. Each descriptor specifies a mapping function $F : \tilde{I}(\rho, \theta) \mapsto M_j(\rho, \theta)$, where $M_j(\rho, \theta) \in \mathbb{R}$ is the parametric map according to the j^{th} textural descriptor, $j = 1, \dots, N_T$. In order to extract information related to the eccentricity, for each column of the parametric maps, a set of basic statistical features (standard deviation, mean, median and maximum values, position of the maximum value, histogram bins) is computed by means of a second mapping function, D :

$$D : M_j(\rho, \theta) \mapsto f_i(\theta) \quad (2)$$

where $f_i(\theta) \in \mathbb{R}$, $i = 1, \dots, N_S$, being N_S the total number of statistical descriptors. Since in this step we are considering radial properties of the image, in order to extract homogeneous features the center of the image has

to coincide with the vessel center. For this reason, the applied rigid registration proves to be a necessary step. Each column (angular sector) θ is then described by a feature vector, obtained by concatenating all the features, $f_i(\theta) = [f_1(\theta) f_2(\theta) \dots f_{N_F}(\theta)]$. The used descriptors are: Gabor filters [4], Local Binary Patterns (LBP) [5] and Cross-correlation between successive frames [6]. The gray-level image is considered as one of the maps, as well. The total number of used features is $N_F = 166$.

We propose the application of the AdaBoost classification algorithm [7] with Decision Stump weak classifier, to implement the classification stage. The main advantages of AdaBoost are its computational simplicity and speed, which make it particularly suitable for clinical applications. Moreover, the classifier is able to work with a large set of features and is not prone to overfitting.

3 Experimental Results

A set of 10 in-vivo pullbacks of human coronary arteries has been acquired with an iLab IVUS Imaging System (Boston Scientific) using a 40 MHz catheter Atlantis SR 40 Pro (Boston Scientific). Each sequence contains an average of 3000 frames, for a total amount of 24 bifurcations. In order to validate our approach, a ground-truth of bifurcation labels has been created by manual segmentation performed by two medical experts. To this aim, an *ad-hoc* interface has been developed. For each pullback, the physicians selected, for each bifurcation, the angle which comprises the bifurcation in the *short-axis view* and the initial and final branching frames in the *longitudinal view*. The procedure for ground-truth collection explains the relevance of the application of a gating technique, which avoids the presence of non-bifurcations samples into a longitudinal vessel segment labeled as bifurcation, otherwise caused by the swinging effect. The ground-truth labels are used for both the training and the validation of the methodology.

The classifier performance is assessed by means of the *Leave-One-Patient-Out* (LOPO) cross-validation technique, over the $N_p = 10$ sequences. At each validation fold, performance is evaluated in terms of accuracy (A), sensitivity (S), specificity (K), precision (P) and false alarm ratio (FAR). The positive and negative classes are strongly unbalanced; therefore, a normalization of the confusion matrix is applied for the computation of all the parameters, with the exception of the accuracy. Given the classification-based nature of the proposed methodology, a comparison with another *state-of-the-art* discriminative classifier is straightforward: we therefore compare the performance of AdaBoost to Random Forest [8]. The AdaBoost classifier has been trained with up to $T = 110$ rounds. The parameters of the Random Forest classifier have been set to a number of trees $N_{trees} = 1000$ and a number of input variables determining the decision at each node, $M_{try} = \log_2 N_F + 1$, as suggested by [8]. Both classifiers have been tuned, during the training process, to optimize the accuracy score, following the standard methodology.

It is worth noticing that in a detection problem, $S = TP / (TP + FN)$ can be regarded as the most relevant parameter, since it expresses the *true positive*

rate (the proportion of actual bifurcation samples which are correctly identified as such). We can therefore consider S as the parameter to maximize in the branching detection problem. The precision $P = TP / (TP + FP)$ (*positive predictive value*) is another relevant parameter, representing the proportion of samples assigned to the bifurcation class which are correctly classified.

The results of the automatic classification are presented in Table 1, together with the inter-observer variability. As it can be observed, for the inter-observer variability the sensitivity is lower than the other parameters, thus demonstrating that even the manual bifurcation location performed by expert physicians is challenging. The results of the AdaBoost automatic classification are superior to manual classification in terms of sensitivity, showing that the algorithm reaches a compromise between the two labeled ground-truths. The Random Forest classifier is ahead of AdaBoost for almost all the considered parameters, with the exception of S , while being comparable with the manual annotation.

In order to corroborate the quality of the achieved results, we perform a statistical analysis. For each pair of approaches, the Wilcoxon signed-ranks test [9] is applied, with a *p-value* $\alpha = 0.05$. Table 2 illustrates, for every comparison, the difference between the mean values of the performance parameters; the asterisk denotes that the difference between the results is statistically significant. The statistical analysis shows that the sensitivity of the AdaBoost classifier is significantly better than both Random Forest and inter-observer variability scores. Moreover, the AdaBoost precision, though lower in mean, is not significantly different from the inter-observer variability. AdaBoost gives a higher false alarm ratio score (+3.55%) than Random Forest, but this drawback is compensated by the high gap in sensitivity (+12.44%). Considering these factors, the AdaBoost classifier turns out as the most appropriate technique for this specific task.

Table 1. Performance of the automatic classifiers and inter-observer variability.

<i>LOPO</i>	<i>AdaBoost</i>	<i>Random Forest</i>	<i>Inter – observer</i>
A	$(94 \pm 4.5)\%$	$(96.78 \pm 3.32)\%$	$(98.77 \pm 0.76)\%$
S	$(75.09 \pm 13.7)\%$	$(62.65 \pm 19.16)\%$	$(61.87 \pm 11.27)\%$
K	$(93.51 \pm 4.71)\%$	$(97.06 \pm 3.46)\%$	$(99.38 \pm 0.39)\%$
P	$(92.56 \pm 3.8)\%$	$(95.96 \pm 3.24)\%$	$(99.05 \pm 0.76)\%$
FAR	$(6.49 \pm 4.71)\%$	$(2.94 \pm 3.46)\%$	$(0.62 \pm 0.39)\%$

Table 2. Difference between the mean performance values $\Delta(\text{mean})$ and statistical significance of the difference assessed with the Wilcoxon signed-ranks test, for the three pairs of approaches.

	<i>AD. vs. R.F.</i>	<i>AD. vs. I.O.</i>	<i>R.F. vs. I.O.</i>
<i>A</i>	-2.78% *	-4.77% *	-1.99% *
<i>S</i>	+12.44% *	+13.22% *	+0.78%
<i>K</i>	-3.55% *	-5.87% *	-2.32% *
<i>P</i>	-3.4% *	-6.49%	-3.09% *
<i>FAR</i>	+3.55% *	+5.87% *	+2.32% *

Figs. 5-d, -e, -f, -g illustrate bifurcation frames corresponding to the sequence longitudinal positions highlighted in Fig. 5-a. Fig. 5-c shows a map reporting the pullback classified by using AdaBoost, while Fig 5-h represents the margin values, produced as an output of the AdaBoost classifier for each classified sample. The margin value indicates how likely a sample is to belong to a class; for this reason, it can be interpreted as an estimate of the probability of bifurcation presence.

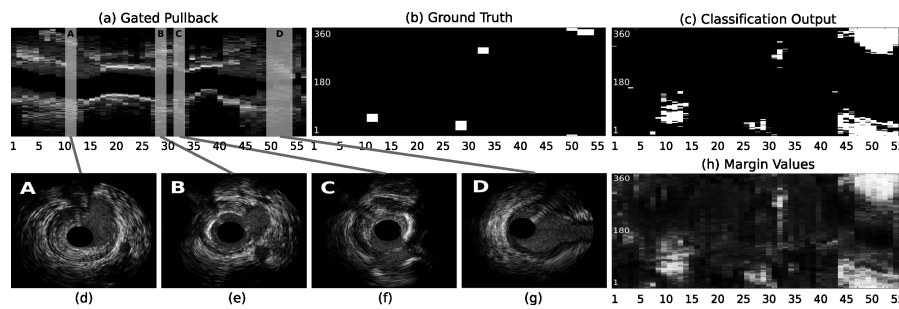


Fig. 5. Pullback after motion artifact compensation (a), ground-truth (b), classification map (c) and map of pseudo-probability of bifurcation presence (h). The maps in (b), (c), (h) represent, on the horizontal and vertical axes, the longitudinal and angular positions along the pullback respectively. In (b) and (c) the white and black colors indicate where bifurcation and non-bifurcation samples (angular sectors) are present, while in (h) pixel intensity represents the probability of bifurcation presence. The frames in (d), (e), (f), (g) correspond to the four bifurcations.

4 Discussion and Conclusion

In this paper, a fully automatic method for the identification of the angular and longitudinal bifurcation position in IVUS sequences is presented. To our knowledge, we are the first to apply bifurcation detection on IVUS images. The novelty of our approach lies in the computation of a set of statistical features on the angular sectors, instead than on the pixels. The task presents a considerable

difficulty, due to the high variability of bifurcation dimensions and appearance in IVUS images. Portions of the vessel can often appear like bifurcations, especially if the blood region is not entirely visible in the image; moreover, bifurcations can be hidden by shadows or change significantly their characteristics in correspondence of implanted stents. Nevertheless, the method shows encouraging results. The current method does not use any kind of feature selection strategy, but future work could deal with a feature selection study, which would reduce the computational cost of the methodology and may improve the results. Since AdaBoost proves to be the most suitable classifier for this problem, the margin value produced as an output can be additionally used to refine the detection results. The spatio-temporal continuity of the bifurcation regions could be considered, by exploiting the neighborhood properties of the angular sector samples. Finally, the feasibility of a study on the estimation of the *angle of incidence* (the angle between the main vessel and the side-branch), will be investigated.

Acknowledgment

This work has been supported in part by projects TIN2009-14404-C02, La Marató de TV3 082131 and CONSOLIDER-INGENIO CSD 2007-00018.

References

1. Zarins, C.K., Giddens, D.P., Bharadvaj, B.K., Sottiurai, V.S., Mabon, R.F., Glagov, S.: Carotid bifurcation atherosclerosis. quantitative correlation of plaque localization with flow velocity profiles and wall shear stress. *Circulation Research* **53** (1983) 502–514
2. Gatta, C., Balocco, S., Ciompi, F., Hemetsberger, R., Rodriguez-Leor, O., Radeva, P.: Real-time gating of ivus sequences based on motion blur analysis: Method and quantitative validation. In: MICCAI (2). (2010) 59–67
3. Gatta, C., Pujol, O., Leor, O.R., Ferre, J.M., Radeva, P.: Fast rigid registration of vascular structures in ivus sequences. *IEEE Transactions on Information Technology in Biomedicine* **13**(6) (2009) 1006–1011
4. Bovik, A., Clark, M., Geisler, W.: Multichannel texture analysis using localized spatial filters. *IEEE Transactions on Pattern Analysis and Machine Intelligence* **12** (1990) 55–73
5. Ojala, T., Pietikäinen, M., Mäenpää, T.: Multiresolution gray-scale and rotation invariant texture classification with local binary patterns. *IEEE Transactions on Pattern Analysis and Machine Intelligence* **24**(7) (2002) 971–987
6. Li, W., van der Steen, A., Lancée, C., Honkoop, J., Gussenhoven, E.J., Bom, N.: Temporal correlation of blood scattering signals in vivo from radio frequency intravascular ultrasound. *Ultrasound in Medicine and Biology* **22**(5) (1996) 583–590
7. Freund, Y., Schapire, R.E.: A decision-theoretic generalization of on-line learning and an application to boosting. *Journal of Computer and System Sciences* **55**(1) (1997) 119–139
8. Statistics, L.B., Breiman, L.: Random forests. In: *Machine Learning*. (2001) 5–32
9. Demsar, J.: Statistical comparisons of classifiers over multiple data sets. *Journal of Machine Learning Research* **7** (2006) 1–30